

A trajectory based understanding of quantum interference

A S Sanz and S Miret-Artés

Instituto de Física Fundamental
Consejo Superior de Investigaciones Científicas
Serrano 123, 28006 Madrid, Spain

E-mail: asanz@imaff.cfmac.csic.es, s.miret@imaff.cfmac.csic.es

Abstract. Interference is one of the most fundamental features defining quantum systems. Here we try to provide a trajectory based analysis of interfering dynamical processes associated with different types of wave-packet superpositions from the standard perspective and a quantum-trajectory based one. From this analysis we obtain clear pictures of the physics behind such quantum processes (of course, always within a quantum-mechanical framework), which can be of general validity to understand more complex cases where interference is crucial (e.g., scattering problems, diffraction by slits or quantum control scenarios).

PACS numbers: 03.65.-w, 03.65.Ta, 03.75.-b, 42.25.Hz

1. Introduction

Over the last 15 years or so, the fields of quantum information theory [1, 2], quantum computation [1, 2] and quantum control [3] have undergone a fast development. At the same time, due to the relevant role that *entanglement* plays in all these fields, the idea that this phenomenon is the most distinctive feature of quantum mechanics has also grown in importance, something that can already be found in Schrödinger's 1935 statement [4, 5]:

“When two systems, of which we know the states by their respective representatives, enter into temporary physical interaction due to known forces between them, and when after a time of mutual influence the systems separate again, then they can no longer be described in the same way, viz. by endowing each of them with a representative of its own. I would not call that *one* but rather *the* characteristic trait of quantum mechanics, the one that enforces its entire departure from classical lines of thought. By the interaction the two representatives (or ψ -functions) have become entangled.”

Nevertheless, despite this relevance, in our opinion *quantum interference* (together with diffraction) can still be considered of more fundamental importance within the quantum theory. Its most striking manifestation is, most surely, the two-slit experiment, which, quoting Feynman [6], “has in it the heart of quantum mechanics. In reality, it contains the *only* mystery.” Quantum interference is the direct, observable consequence of the *coherent* superposition of (quantum) probability fields. This is precisely what is special about it: interferences in quantum mechanics are not associated to or produced by a physical magnitude, as in classical wave mechanics —remember that classical waves are manifestations of the propagation of energy (a physical magnitude) throughout a material medium, or, in other words, the perturbation of such a medium by an energy transfer. But quantum interference is not only important at a conceptual and fundamental level; it is involved in a very wide range of experimental situations and applications, such as SQUIDs or superconducting quantum interference devices [7], the coherent control of chemical reactions [3], atom and molecular interferometry [8] (in particular, with BECs [9–11], where different techniques to recombine the split beams are used [12–15]), or the Talbot effect with relatively heavy particles (e.g., Na atoms [16] and BECs [17]), just to cite some examples. Moreover, on the other hand, it is also important to mention the important role that interference can play when dealing with multipartite entangled systems as an indicator of the loss of coherence induced by the interaction between the subsystems, for instance.

Despite quantum interference seems to be nowadays a very well known phenomenon, we think that there is still an incompleteness in the full interpretation of interference phenomena. This lack is associated to the physical “reality” ascribed to the superposition principle on which interference is grounded. According to this (mathematical) principle, wave fields can be decomposed and then recombined again to produce and explain interferences. However, in Nature, wave fields are a whole and,

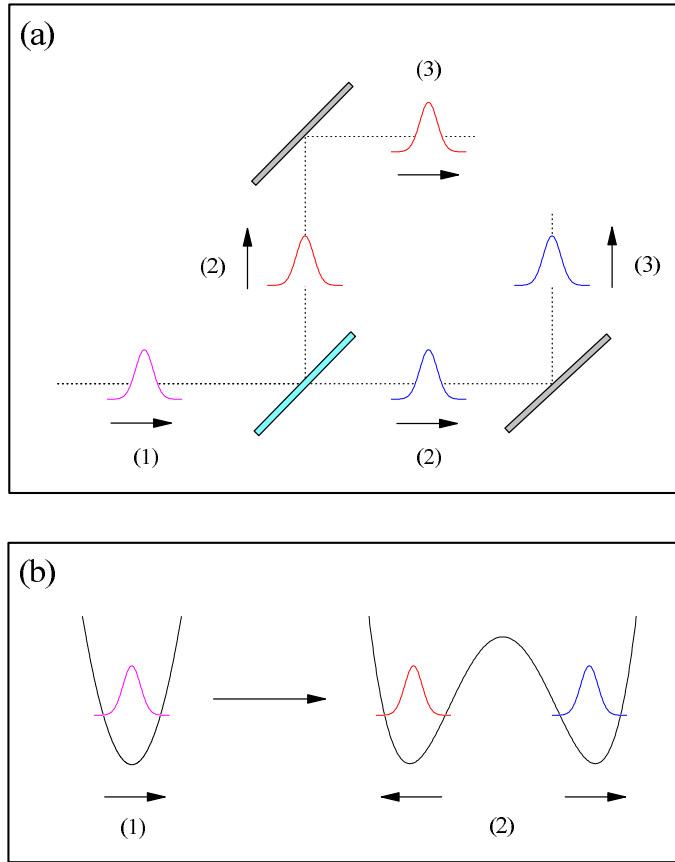


Figure 1. Two situations where the wave function describing the system can be described in terms of a two wave-packet superposition. (a) After reaching a beam-splitter, an incoming wave packet (1) splits into two wave packets (2). These wave packets move apart until they reach two reflectant mirrors, which redirect their propagation (3) in such a way that, after some time, they will “collide”, displaying interference. (b) A wave packet confined in a potential well (1) is split into two wave packets by creating a barrier inside the potential (2) and then pulling outwards the two new potential wells (each containing a new wave packet). After these wave packets are separated, the potential can be turned off and then control the propagation of such wave packets to make them to interfere, as happens in Bose-Einstein interferometric techniques.

therefore, it is important to determine what this behavior means when we are dealing with quantum systems displaying interference. This is our main purpose in the present work, where we analyze such consequences in the case of coherent superpositions of Gaussian wave packets by means of the hydrodynamical picture of quantum mechanics, namely Bohmian mechanics [18, 19]. Rather than simple academical examples, such superpositions are experimentally realizable (and, indeed, used) in atom interferometry [12–15]; in Fig. 1, for instance, we have sketched two types of experiments where coherent superpositions of Gaussian wave packets can be produced. We work here with this particular type of superpositions because their interference dynamics is well known in both standard quantum mechanics and Bohmian mechanics [20, 21], which will be of much help to understand and interpret the results presented as well as to extrapolate

them to more complicated contexts. Apart from the fundamental-like character of this work, we would like to highlight the complementary understanding of quantum physics that Bohmian mechanics provides in scattering processes and (quantum) control scenarios, as well as its great help in the new design, development, improvement and/or implementation of trajectory-based algorithms [22].

The organization of this work is as follows. We will start our discussion, in section 2, by introducing the problem of the interpretation of the superposition principle from both the standard quantum-mechanical viewpoint and the Bohmian one, and considering general wave functions. As shown, Bohmian mechanics allows one to break the ambiguity introduced for many years by the standard quantum mechanics due to its description of wave phenomena in terms of the trajectories associated with the associate quantum probability flows. To illustrate our assertions, several representative cases are analyzed next, in section 3. Finally, the main conclusions derived from this work are summarized and discussed in section 4.

2. Interference and quantum trajectories

It is well known that the solutions of the one-dimensional time-dependent Schrödinger equation,

$$i\hbar \frac{\partial \Psi}{\partial t} = -\frac{\hbar^2}{2m} \frac{\partial^2 \Psi}{\partial x^2} + V\Psi \quad (1)$$

satisfy the superposition principle. That is, given ψ_1 and ψ_2 satisfying separately Eq. (1), we can construct

$$\Psi(x, t) = \psi_1(x, t) + \psi_2(x, t) \quad (2)$$

which is also a solution of this equation. These solutions are known to be *dispersive* since they cannot be expressed as $\Psi(x - vt)$, like the solutions of the classical wave equation, even in the case $V(x) = 0$ —with the exception of the non-dispersive Airy wave packets [23]. More important is, however, the fact that, unlike classical waves, the wave amplitude Ψ is not an *observable* magnitude, but its square modulus, $\rho = |\Psi|^2$, namely the *probability density*. According to Born [24], ρ provides a statistical description of the system. Due to the connection between Ψ and ρ , it is clear that the superposition principle does not hold for the latter. Note that, expressing ψ_i ($i = 1, 2$) in polar form, i.e., $\psi_i(x, t) = \rho_i^{1/2}(x, t)e^{iS_i(x, t)/\hbar}$, we find

$$\rho = \rho_1 + \rho_2 + 2\sqrt{\rho_1\rho_2} \cos \varphi, \quad (3)$$

where

$$\varphi = \frac{S_2 - S_1}{\hbar}. \quad (4)$$

The interference term in Eq. (3) connects *coherently* the probabilities (ρ_1 and ρ_2) related to each partial wave (ψ_1 and ψ_2 , respectively).

Since ρ describes the statistical distribution associated with a particle ensemble regardless of whether there is an interaction potential connecting them or not (i.e.,

we are are describing identical ensembles or multipartite systems), one can define an associate probability current density as

$$\mathbf{J}(\mathbf{r}, t) = \frac{1}{m} \operatorname{Re} [\Psi^*(\mathbf{r}, t) \hat{\mathbf{p}} \Psi(\mathbf{r}, t)] = -\frac{i\hbar}{2m} [\Psi^* \nabla \Psi - \Psi \nabla \Psi^*], \quad (5)$$

which indicates the flow of such ensembles, with $\hat{\mathbf{p}} = -i\hbar \nabla$ being the momentum (vector) operator. Substituting (2) into (5), with each partial wave function ψ_i also expressed in polar form, we obtain

$$\mathbf{J} = \frac{1}{m} \left[\rho_1 \nabla S_1 + \rho_2 \nabla S_2 + \sqrt{\rho_1 \rho_2} \nabla (S_1 + S_2) \cos \varphi + \hbar (\rho_1^{1/2} \nabla \rho_2^{1/2} - \rho_2^{1/2} \nabla \rho_1^{1/2}) \sin \varphi \right], \quad (6)$$

which clearly shows that the superposition principle does not hold either for \mathbf{J} . The two magnitudes ρ and \mathbf{J} are related through the continuity equation,

$$\frac{\partial \rho}{\partial t} + \nabla \cdot \mathbf{J} = 0, \quad (7)$$

which can be easily derived from Eq. (1) after multiplying both sides by Ψ^* , adding to the resulting equation its complex conjugate, and then rearranging terms.

Within this hydrodynamical picture of quantum mechanics [25] —arising when this theory is recast in terms of the (hydrodynamical) fields ρ and \mathbf{J} —, one can always further proceed and determine the probability streamlines, i.e., the lines along which the probability flows. Consider the same polar ansatz used above, but for the total wave function Ψ ,

$$\Psi(\mathbf{r}, t) = \rho^{1/2}(\mathbf{r}, t) e^{iS(\mathbf{r}, t)/\hbar}. \quad (8)$$

After substituting (8) into (1) and rearranging terms, one obtains

$$\frac{\partial S}{\partial t} + \frac{(\nabla S)^2}{2m} + V + Q = 0 \quad (9)$$

$$\frac{\partial \rho}{\partial t} + \frac{1}{m} \nabla \cdot (\rho \nabla S) = 0 \quad (10)$$

from the real and imaginary parts of the resulting expression, respectively. Equation (10) is the continuity equation (7), with $\mathbf{J} = (\rho \nabla S)/m$. Equation (9), more interesting from a dynamical viewpoint, is the quantum Hamilton-Jacobi equation, which allows us to reinterpret the whole quantum-mechanical formalism in terms of the eventual paths that the system can pursue when it is considered as a particle. These paths are defined as solutions of the equation of motion

$$\dot{\mathbf{r}} = \frac{\nabla S}{m} = \frac{\mathbf{J}}{\rho} = -\frac{i\hbar}{2m} \frac{\Psi^* \nabla \Psi - \Psi \nabla \Psi^*}{\Psi^* \Psi}, \quad (11)$$

where S represents a quantum generalized action. Within this formulation, quantum trajectories are then the characteristics associated with S —i.e., the *rays* perpendicular to the surfaces of constant S at each time. Note that considering Eq. (11) means to introduce a new conceptual element into the quantum-mechanical formalism: the presence of well-defined trajectories in both space and time. This new element constitutes the essence of what is known nowadays as Bohmian mechanics [18, 19], a quantum mechanics based on the hydrodynamical Eqs. (9) and (10) plus the particle

equation of motion (11). As infers from this set of equations, the difference with respect to classical mechanics is that trajectories not only evolve under the action of an external potential V , but also are affected by the so-called *quantum potential*

$$Q = -\frac{\hbar^2}{2m} \frac{\nabla^2 \rho^{1/2}}{\rho^{1/2}}, \quad (12)$$

which introduces into the quantum motion the context-dependence and nonlocality necessary for the particles (distributed initially according to $\rho(\mathbf{r}, 0)$) to reproduce the patterns of standard quantum mechanics when they are considered in a large statistical number. The quantum dynamics is thus ruled by a total effective potential $V_{\text{eff}}(\mathbf{r}, t) = V(\mathbf{r}, t) + Q(\mathbf{r}, t)$.

As is apparent from Eqs. (9) to (11), in Bohmian mechanics a system always consists of a wave and a particle; the wave satisfies the hydrodynamical equations (or, equivalently, the time-dependent Schrödinger equation) and the particle is guided by the action of the wave via (11). Because of this relationship between particles and waves, the initial particle momentum is predetermined by $\Psi(\mathbf{r}, 0)$ and therefore it is not necessary to inquire about its value. Only initial positions are freely (and randomly) to be chosen, with the constraint that their distribution is given by $\rho(\mathbf{r}, 0)$. On the other hand, we would also like to stress that Eq. (11) is well defined provided that the wave function is continuous and differentiable. In the case of *quantum fractals* [26] (wave functions which present fractal topologies), one can still obtain (fractal) quantum trajectories by redefining Eq. (11) conveniently [27].

An interesting property of the quantum potential can be found when one computes the energy expected value,

$$\bar{E} = \langle \hat{H} \rangle = \langle \hat{T} \rangle + \langle \hat{V} \rangle, \quad (13)$$

which, in Bohmian mechanics, just consists of determining the ensemble average energy. The first term in (13) is the expected value of the kinetic energy, with $\hat{T} = -(\hbar^2/2m)\nabla^2$ denoting the kinetic operator. When the polar ansatz of the wave function is considered, we obtain

$$\langle \hat{T} \rangle = -\frac{\hbar^2}{2m} \int R \left[\nabla^2 R - \frac{R}{\hbar^2} (\nabla S)^2 \right] d\mathbf{r} + \frac{\hbar}{2im} \int \nabla(\rho \nabla S) d\mathbf{r}. \quad (14)$$

From (10), we have

$$\int \nabla \mathbf{J} d\mathbf{r} = - \int \frac{\partial \rho}{\partial t} d\mathbf{r} = - \frac{\partial}{\partial t} \int \rho d\mathbf{r} = 0, \quad (15)$$

since the probability density conserves in the whole space. In other words, if the system is closed, no probability can flow towards or from the region where this system is defined; this is the probabilistic analog of the energy conservation principle. Therefore, (14) and (13) become

$$\langle \hat{T} \rangle = \int \left(-\frac{\hbar^2}{2m} \frac{\nabla^2 R}{R} \right) \rho d\mathbf{r} + \int \frac{(\nabla S)^2}{2m} \rho d\mathbf{r} = \langle Q \rangle + \frac{\langle p^2 \rangle}{2m} \quad (16)$$

and

$$\bar{E} = \bar{E}_k + \bar{Q} + \bar{V} = \bar{E}_k + \bar{V}_{\text{eff}}, \quad (17)$$

respectively, where \bar{E}_k is the average (expected value) contribution from the kinetic energy associated with each particle from the ensemble. Thus, notice that, although Q is usually assigned the role of a quantum potential energy, since it is obtained from the kinetic operator and contributes to the expected value of the kinetic energy, one can also consider it as a quantum kinetic energy. More importantly, putting aside such considerations, Q is the only responsible for making quantum dynamics so different from classical ones due to its nonlocal nature (\bar{E}_k and \bar{V} only contain local information) —note that Q contains information about the whole quantum state and therefore supplies it to the particle at the particular point where it is located. From a practical or computational point of view, this explains why a good representation of the momentum operator has to contain a wide spectrum of momenta. Furthermore, (17) also indicates that classical-like behaviors appear whenever the part of the energy associated with the quantum potential becomes sufficiently small.

To conclude this section, we are going to note another interesting property of quantum motion: in Bohmian mechanics two trajectories cannot cross the same point at the same time in the configuration space (note that, in classical mechanics, this only happens in the phase-space). In order to prove this, consider that two velocities are assigned to the same point \mathbf{r} , $v_1(\mathbf{r})$ and $v_2(\mathbf{r})$, with $v_1 \neq v_2$. From (11) we know that these velocities are directly related to some wave functions $\psi_1(\mathbf{r})$ and $\psi_2(\mathbf{r})$, respectively. If both wave functions are solutions of the same Schrödinger equation, the only possibility for them to be different on the same point x is that their phases differ, as much, in a time-dependent function (and/or space-independent constant), i.e.,

$$S_2(\mathbf{r}, t) = S_1(\mathbf{r}, t) + \phi(t). \quad (18)$$

Now, since the velocities are the gradient of these functions, it is clear that v_2 has to be equal to v_1 necessarily (of course, we are assuming that the wave functions do not vanish on \mathbf{r}).

3. Simple examples of quantum interference with Gaussian wave packets

3.1. The free Gaussian wave packet

Since we will consider wave functions consisting of one-dimensional superpositions of Gaussian wave packets, let us first briefly overview the case of a free Gaussian wave packet. Such a wave packet, which satisfies (1), can be expressed as

$$\Psi(x, t) = A_t e^{-(x-x_t)^2/4\tilde{\sigma}_t\sigma_0 + ip(x-x_t)/\hbar + iEt/\hbar}, \quad (19)$$

where $A_t = (2\pi\tilde{\sigma}_t^2)^{-1/4}$ and the complex time-dependent spreading is

$$\tilde{\sigma}_t = \sigma_0 \left(1 + \frac{i\hbar t}{2m\sigma_0^2} \right). \quad (20)$$

From (20), the spreading of this wave packet at time t is

$$\sigma_t = |\tilde{\sigma}_t| = \sigma_0 \sqrt{1 + \left(\frac{\hbar t}{2m\sigma_0^2} \right)^2}. \quad (21)$$

Due to the free motion, $x_t = x_0 + v_p t$ ($v_p = p/m$ is the propagation velocity) and $E = p^2/2m$, i.e., the centroid of the wave packet moves along a classical rectilinear trajectory. This does not mean, however, that the expected (or average) value of the wave-packet energy is equal to E , which, according to Eq. (17), results

$$\bar{E} = \frac{p^2}{2m} + \frac{\hbar^2}{8m\sigma_0^2}. \quad (22)$$

In (22) we thus observe two contributions. The first one is associated with the propagation or translation of the wave packet, while the latter is related to its spreading and has, therefore, a purely quantum-mechanical origin. From now on, we will denote them as E_p and E_s , respectively. Note that neither E_p nor E_s , and therefore \bar{E} , depend on time. Expressing E_s in terms of an *effective* momentum p_s (i.e., $E_s = p_s^2/2m$), we find

$$p_s = \frac{\hbar}{2\sigma_0}, \quad (23)$$

which resembles Heisenberg's uncertainty principle. This allows us to refer the wave-packet dynamics to two well-defined velocities: v_p and v_s .

The relationship between v_p and v_s plays an important role in the type of effects that one can observe when dealing with wave packet superpositions. To better understand this statement, consider Eq. (21). Defining the timescale

$$\tau = 2m\sigma_0^2/\hbar, \quad (24)$$

we find that, if $t \ll \tau$, the width of the wave packet remains basically constant with time, $\sigma_t \approx \sigma_0$ (i.e., for practical purposes, it is roughly time-independent up to time t). On the contrary, if $t \gg \tau$, the width of the wave packet increases linearly with time ($\sigma_t \approx \hbar t/2m\sigma_0$). Of course, in between there is a smooth transition; from (21) it is shown that the progressive increase of σ_t describes a hyperbola when this magnitude is plotted *vs* time. These are “dynamical” relationships in the sense that the dynamical behavior of the wave packet is known comparing the actual time t with the effective time τ . When we are dealing with general wave packets, *a priori* we do not have an effective time τ to compare with. This inconvenience can be avoided if we consider the interpretive framework provided by v_p and v_s , which can be estimated from the initial state through Eq. (16). Within this framework, we can find a way to know which process—spreading or translational motion—is going to determine the wave packet dynamics, as follows. Expression (21) can be rewritten in terms of v_s as

$$\sigma_t = |\tilde{\sigma}_t| = \sigma_0 \sqrt{1 + \left(\frac{v_s t}{\sigma_0}\right)^2}. \quad (25)$$

Now, consider that t is the time that takes the wave-packet centroid to cover a distance $d = v_p t \approx \sigma_0$. Introducing this result into (25), we obtain

$$\sigma_t = |\tilde{\sigma}_t| = \sigma_0 \sqrt{1 + \left(\frac{v_s}{v_p}\right)^2}. \quad (26)$$

This time-independent expression shows that, only using information about the initial preparation of the wave packet, we can obtain information on its subsequent dynamical behavior. Thus, $t \ll \tau$ is equivalent to having an initial wave packet prepared with $v_s \ll v_p$: the translational motion will be much faster than the spreading of the wave packet. On the other hand, $t \gg \tau$ is equivalent to $v_s \gg v_p$: the wave packet spreads very rapidly in comparison with its advance along x .

In order to better understand the “competition” between v_p and v_s , note that, introducing (19) into (11) and integrating in time, we find [28]

$$x(t) = v_p t + \frac{\sigma_t}{\sigma_0} x_0. \quad (27)$$

The short-time limit is not very interesting: Bohmian trajectories are basically parallel to classical ones, since $x(t) \approx x_0 + v_p t$. However, in the long-time limit we have

$$x(t) \approx \left(v_p + v_s \frac{x_0}{\sigma_0} \right) t. \quad (28)$$

Since the maximum values of $|x_0|$ are of the order of σ_0 , $|x_0|/\sigma_0 \approx 1$ and the trajectory dynamics will be ruled by both v_p and v_s , in general. Depending on which velocity is larger, the dynamics will be more strongly influenced by one process or the other, as said above. If v_p is dominant, the asymptotic motion is basically a classical like motion (no appreciable spreading in comparison with the distances covered by particles). However, if v_s is dominant, although the motion is classical-like (i.e., there is an asymptotic constant velocity, v_s), it has a purely quantum-mechanical origin and therefore eventual effects produced within this regime will also be purely quantum-mechanical.

3.2. Dynamics of coherent wave-packet superpositions

Slit experiments —e.g., the double-slit experiment— and interferometric experiments —e.g., BEC interferometry— essentially constitute the two types of contexts where one can find interference from coherent superpositions of quantum states associated with material particles. In the first case, after an incident beam is diffracted by the slits, the interference of the outgoing beams (which are coherent because they arise from the same source) causes the well-known diffraction patterns. In the latter case, the interference is produced during the period of time where both beams (which are also coherent regardless of how the beams have been created) coincide at a certain space region. While the final pattern in the first case constitutes a sort of “collective” effect, where there is no clue on each partial beam, in the second case the two beams emerge after the interference. According to these different final, asymptotic behaviors, we can generically denote these experiments as diffraction-like and collision-like, respectively. As shown below, these behaviors are associated with the ratio between the velocities v_p and v_s described in the previous section: a typical diffraction-like experiment is characterized by $v_p \ll v_s$, while for collision-like experiments we have $v_p \gg v_s$.

Consider a general coherent superposition of two Gaussian wave packets. If no external potential is applied ($V = 0$), the wave function describing this superposition

can be expressed at any time as

$$\Psi(\mathbf{r}, t) = c_1 \psi_1(\mathbf{r}, t) + c_2 \psi_2(\mathbf{r}, t), \quad (29)$$

where the partial waves ψ_i are normalized Gaussian wave packets, like (19), propagating with opposite velocities. We also assume that, initially, the centers of these wave packets are far enough in order to minimize their overlapping in the region between them — i.e., $\rho_1(\mathbf{r}, 0)\rho_2(\mathbf{r}, 0) \approx 0$. With this condition, the weighting factors c_1 and c_2 satisfy the relation $|c_1|^2 + |c_2|^2 = 1$. As will be shown below, these factors also influence the topology of the quantum trajectories —as well as the v_p/v_s ratio—, therefore we will reexpress (29) more conveniently as

$$\Psi(\mathbf{r}, t) = c_1 [\psi_1(\mathbf{r}, t) + \sqrt{\alpha} \psi_2(\mathbf{r}, t)], \quad (30)$$

where

$$\alpha = \frac{c_2^2}{c_1^2} = \frac{1}{c_1^2} - 1. \quad (31)$$

This allows us to express the probability density and the quantum current density as

$$\rho = c_1^2 [\rho_1 + \alpha \rho_2 + 2\sqrt{\alpha} \sqrt{\rho_1 \rho_2} \cos \varphi], \quad (32)$$

$$\begin{aligned} \mathbf{J} = \frac{c_1^2}{m} & \left[\rho_1 \nabla S_1 + \alpha \rho_2 \nabla S_2 + \sqrt{\alpha} \sqrt{\rho_1 \rho_2} \nabla (S_1 + S_2) \cos \varphi \right. \\ & \left. + \hbar \sqrt{\alpha} (\rho_1^{1/2} \nabla \rho_2^{1/2} - \rho_2^{1/2} \nabla \rho_1^{1/2}) \sin \varphi \right], \end{aligned} \quad (33)$$

respectively. Also, substituting (32) and (33) into (11), we can obtain the associate quantum trajectories from the equation of motion

$$\begin{aligned} \dot{\mathbf{r}} = \frac{1}{m} & \frac{\rho_1 \nabla S_1 + \alpha \rho_2 \nabla S_2 + \sqrt{\alpha} \sqrt{\rho_1 \rho_2} \nabla (S_1 + S_2) \cos \varphi}{\rho_1 + \alpha \rho_2 + 2\sqrt{\alpha} \sqrt{\rho_1 \rho_2} \cos \varphi} \\ & + \sqrt{\alpha} \frac{\hbar}{m} \frac{(\rho_1^{1/2} \nabla \rho_2^{1/2} - \rho_2^{1/2} \nabla \rho_1^{1/2}) \sin \varphi}{\rho_1 + \alpha \rho_2 + 2\sqrt{\alpha} \sqrt{\rho_1 \rho_2} \cos \varphi}. \end{aligned} \quad (34)$$

In this expression there are two well-defined contributions, which can be related to the effects caused by the interchange of the wave packets (or the associate partial fluxes) on the particle motion (specifically, on the topology displayed by the corresponding quantum trajectories); note that the first contribution is even after interchanging only the modulus or only the phase of the wave packets, while the second one changes its sign with these operations. From the terms that appear in each contribution, it is apparent that the first contribution is associated with the evolution of each individual flux as well as with their combination. Thus, it provides information about both the asymptotic behavior of the quantum trajectories and also about the interference process (whenever the condition $\rho_1(\mathbf{r}, t)\rho_2(\mathbf{r}, t) \approx 0$ is not satisfied). On the other hand, the second contribution describes interference effects connected with the asymmetries or differences of the wave packets. For instance, their contribution is going to vanish if they are identical and coincide on $x = 0$ although their overlapping is nonzero.

Let us first consider the collision-like case, where, for the sake of simplicity and without loss of generality, we will assume $\alpha = 1$ and that both wave packets are identical,

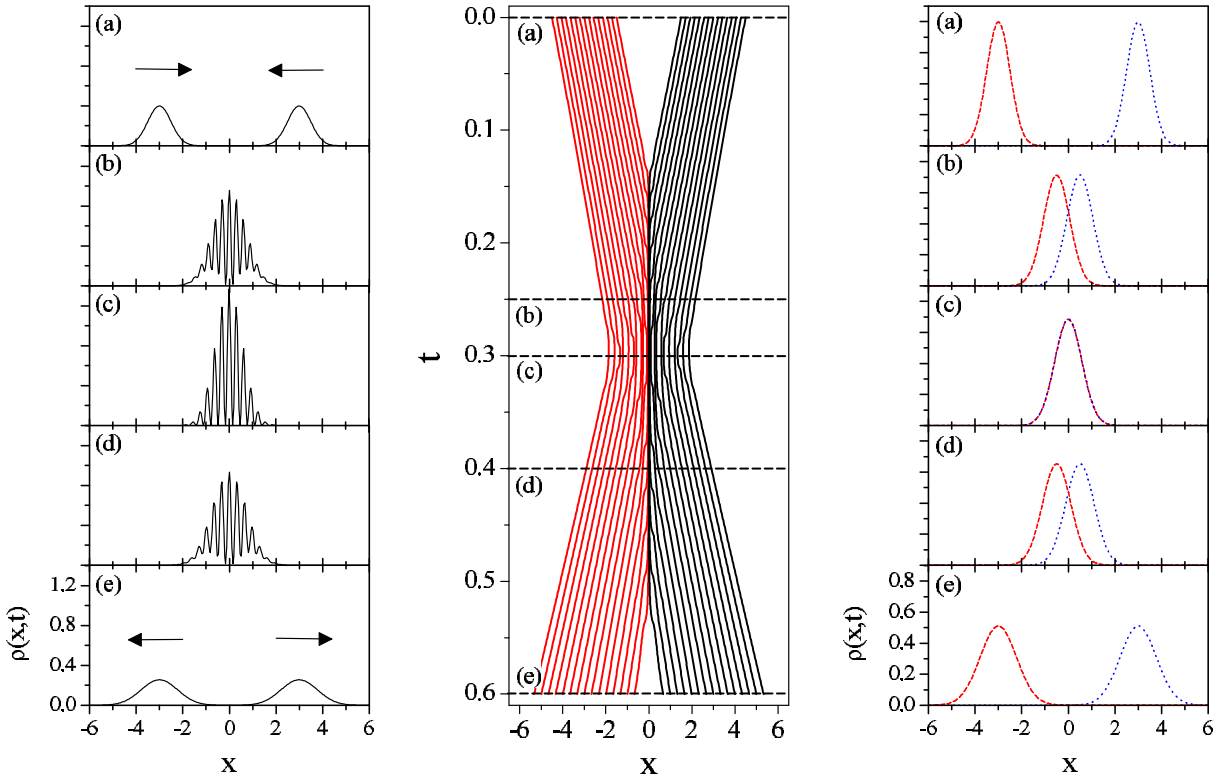


Figure 2. Left: From (a) to (d), snapshots illustrating the time-evolution of two colliding Gaussian wave packets, with $v_p = 10$ and $v_s = 1$. Center: The same process as in the left column, by visualized in terms of quantum trajectories. The perpendicular dashed lines mark cuts in time corresponding with the same labels as in the figures of the left column. Right: Interpretation of the process in the left column according to the quantum trajectories shown in the central column.

propagate in opposite directions. Moreover, also for simplicity in the discussion, we will refer to the regions where ψ_1 and ψ_2 are launched from as I and II, respectively. In standard quantum mechanics, a physical reality is assigned to the superposition principle, which in this case means that, after the wave packets have maximally interfered at t_{\max}^{int} (panel (c) in the left column of Fig. 2), ψ_1 moves to region II and ψ_2 to region I. As mentioned above, the wave packets (or, more specifically, their associate probability densities) represent the statistical behavior of a swarm of quantum particles distributed accordingly. Therefore, according to the standard view arising from the superposition principle, one should start to observe crossings between trajectories in a certain time range around t_{\max}^{int} . However, this is not the behavior displayed by the Bohmian trajectories displayed in the central panel of Fig. 2, which avoid such crossings during the time range where interference effects are important. Note that quantum-mechanical statistics are characterized by keeping the coherence and transmitting it to the corresponding quantum dynamics, as infers from Eq. (34). Thus, the interference process has to be interpreted in a different way (than the standard quantum-mechanical one) when it is analyzed from a quantum trajectory perspective. As inferred from

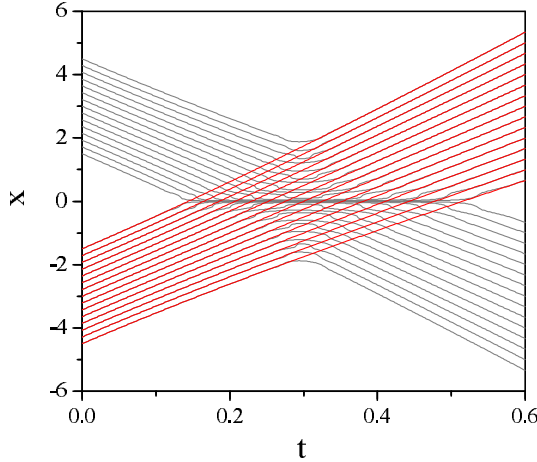


Figure 3. Bohmian trajectories associated with a Gaussian wave-packet superposition (grey) and a single Gaussian wave packet (red). As shown, the presence of the other wave packet makes the dynamics to avoid the crossing in the central part; the asymptotic part remains being the same as without presence of other wave packet. Here $v_p = 10$ and $v_s = 1$.

Eq. (34), for identical (but counter-propagating) wave packets, the velocity field vanishes along $x = 0$ at any time. This means that there cannot be any probability density (or particle) flux between regions I and II at any time. Therefore, trajectories starting in one of these regions will never cross to the other one and vice versa. Hence the final outgoing wave packets in panel (e) in the left column of Fig. 2 necessarily describe exactly the same swarms of particles associated with the wave packets that we had in their respective regions initially (see panel (a) of the same figure). The whole process can be understood them as a sort of bouncing back of the wave packets once they have reached the intermediate position between them, as schematically represented in the right column of Fig. 2.

But, if the two swarms of trajectories do not cross each other, why the swarm associated initially with one of the wave packets behaves asymptotically as associated with the other one, as seen in Fig. 3? According to the standard description based on the superposition principle, the wave packets cross. This can be understood as a transfer or interchange of probabilities from region I to region II and vice versa. On the other hand, from a dynamical (quantum trajectory) viewpoint, this also means that the sign of the associate velocity field will change after the collision. That is, before the collision its sign points onwards (towards $x = 0$) and after the collision it points outwards (diverging from $x = 0$) —at t_{\max}^{int} it does not point anywhere, but remains *steady*. Thus, like in a particle-particle elastic scattering process particles exchange their momenta, here the swarms of particles will exchange their probability distributions “elastically”. This is nicely illustrated in Fig. 3: after the collision, the two swarms of trajectories (grey lines) bounce backwards and follow the paths that they would be pursued by the non deflected particles (red lines). We can describe this process analytically as follows.

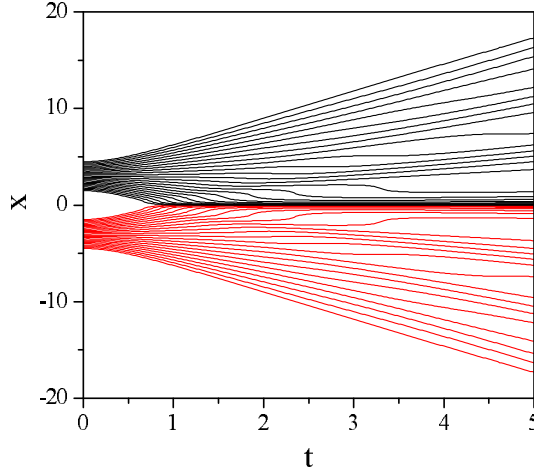


Figure 4. Bohmian trajectories associated with a Gaussian wave-packet superposition with $v_p = 0.1$ and $v_s = 1$. Unlike the case shown in Figs. 2 and 3, here the spreading of both wave packets is much faster than their translational motion, thus giving rise to the observation of an interference-like final outcome.

Initially, depending on the region where the trajectories are launched from, they are described approximately by

$$\dot{\mathbf{r}}_I \approx \nabla S_1/m \quad \text{or} \quad \dot{\mathbf{r}}_{II} \approx \nabla S_2/m. \quad (35)$$

Now, asymptotically (for $t \gg t_{\max}^{\text{int}}$), Eq. (34) can be expressed as

$$\dot{\mathbf{r}} \approx \frac{1}{m} \frac{\rho_1 \nabla S_1 + \rho_2 \nabla S_2}{\rho_1 + \rho_2}, \quad (36)$$

where we make use of the approximation $\rho_1(\mathbf{r}, t)\rho_2(\mathbf{r}, t) \approx 0$. Note that this approximation also means that the total probability density, $\rho = \rho_1 + \rho_2$, is nonzero only on ρ_1 or ρ_2 . Specifically, in region I we will have $\rho \approx \rho_2$ and in region II, $\rho \approx \rho_1$. When this result is introduced into Eq. (36), we finally obtain

$$\dot{\mathbf{r}}_I \approx \nabla S_2/m \quad \text{and} \quad \dot{\mathbf{r}}_{II} \approx \nabla S_1/m, \quad (37)$$

which reproduce the dynamics observed asymptotically. This trajectory picture thus provides us with a totally different interpretation of wave packet interference with respect to the standard one: although probability distributions transfer, particles remain always within the domains defined by their corresponding initial distributions (which have been here as regions I and II). The *non-crossing* property of Bohmian mechanics (see section 2) thus makes apparent the constraint that exists for the quantum probability flux, which goes beyond the separability of fluxes implicit in the superposition principle.

Now we are going to consider the diffraction-like case, where the dominant effect is the overlapping of the two wave packets due to their fast spreading. This means that no individual wave packet can be then distinguished asymptotically. The quantum trajectories corresponding to this case are displayed in Fig. 4. Note that although asymptotically the trajectories are straight lines in the the so-called *Fraunhofer region*

[20, 29], their corresponding asymptotic momenta are quantized and have nothing to do with the initial ones associated with ψ_1 and ψ_2 ($p_{01} = p$ and $p_{02} = -p$, respectively), unlike the collision-like case. These quantized momenta arise from the phase difference between S_1 and S_2 , which produces periodic oscillations of the final diffraction pattern due to the (also periodic) accumulation of trajectories in particular space regions — this effect is much more noticeable as the number of beams in the superposition increases [20, 21]. This asymptotic effect can also be explained analytically as follows. Within the Fraunhofer region, both ρ_1 and ρ_2 are sufficiently spread as to consider that they are flat (i.e., $\nabla\rho_i \approx 0$) for practical purposes. This allows us to use the approximation $\rho_1 \approx \rho_2 \approx \rho_0$ for all x . Thus, after also considering the approximation $v_p \sim 0$ when compared with v_s , we obtain

$$\rho \approx 4\rho_0 \cos^2(\varphi/2), \quad (38)$$

$$\varphi \approx -\frac{m\ell x}{\hbar t}, \quad (39)$$

where $\ell = |x_{02} - x_{01}| = 2x_0$ ($x_{02} = x_0 = -x_{01}$). It is clear that ρ will present maxima whenever $\varphi/2 = n\pi$ or, equivalently,

$$\frac{x}{t} = 2\pi n \left(\frac{\hbar}{m\ell} \right) = 2\pi n v_s \left(\frac{\sigma_0}{x_0} \right), \quad (40)$$

with $n = 0, \pm 1, \pm 2, \dots$ being the so-called *diffraction order*. Now, applying the same approximation to Eq. (34), we find

$$\dot{x} \approx \frac{\nabla S_1 + \nabla S_2}{2m} \approx \frac{x}{t} = \pm 2\pi n v_s \left(\frac{\sigma_0}{x_0} \right). \quad (41)$$

The solutions of this equation of motion are obtained by direct integration and have the general form

$$x(t) \approx \pm 2\pi n \frac{\sigma_0}{x_0} (v_s t), \quad (42)$$

i.e., the asymptotic solutions of Eq. (34) in the problem of the two Gaussian wave packets follow straight lines, whose slopes are quantized quantities (through n) which are proportional to the spreading velocity v_s . In the exact problem, displayed in Fig. 4, we observe that the trajectories associated with a certain diffraction channel (characterized by a quantized momentum $2\pi n(\sigma_0/x_0)p_s$) distribute around the respective asymptotic value, given by (42). This value represents the average of all quantum trajectories when they are correspondingly weighted, i.e., when the initial weight corresponding to each trajectory ($\rho_0(x_0)$, with x_0 being the trajectory initial condition) is taken into account in the averaging process associated with that diffraction channel [29].

3.3. Asymmetric coherent superpositions

In the previous section we have studied interference processes with identical Gaussian wave packets propagating symmetrically with respect to $x = 0$. However, what happens in other more general situations where neither the wave packets are identical nor their

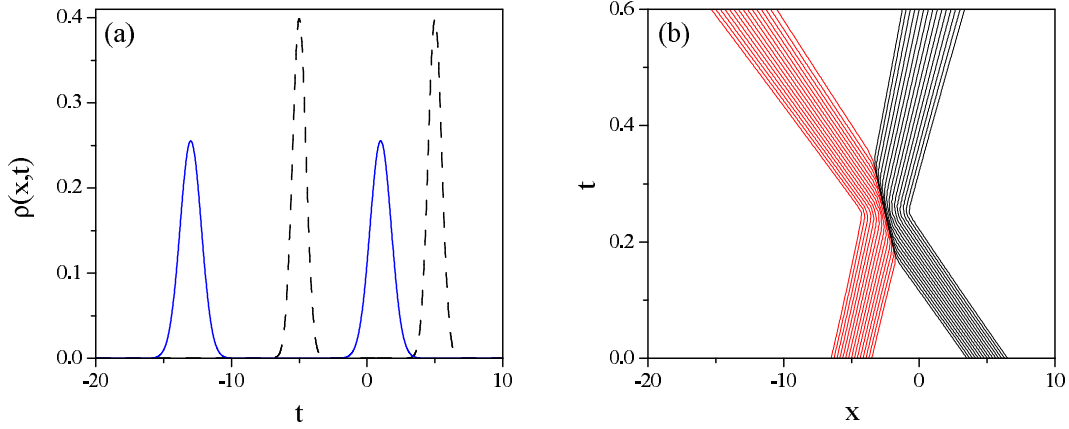


Figure 5. (a) Probability density at $t = 0$ (black-dashed line) and $t = 0.6$ (blue-solid line) for a wave packet superposition with $p_{01} = 10$ and $p_{02} = -30$. The value of the other relevant parameters are $\sigma_{01} = \sigma_{02} = 0.5$ and $\alpha = 1$. (b) Quantum trajectories associated with the dynamics described by the situation displayed in panel (a).

weights? Although one could think of many different possibilities, it is enough to consider three cases in order to already obtain an insight on the related physics. The criterion followed to classify these cases is based on which property of the wave packets is varied (with respect to the symmetric case described in section 3.2) or considered at a time:

- A) Different modulus of the initial average momentum ($|p_{01}| \neq |p_{02}|$).
- B) Different initial spreading ($\sigma_{01} \neq \sigma_{02}$).
- C) Different weights ($c_1 \neq c_2$ or, equivalently, $\alpha \neq 1$).

Since the collision-like case is simpler to understand than the diffraction-like one, below we will assume $v_p \gg v_s$, although generalizing to any v_p/v_s ratio is straightforward. Moreover, as before, the initial distance between both wave packets is such that the initial overlapping is negligible.

Case A is represented in Fig. 5, where we can observe that varying the moduli of the initial average momenta only produces an asymmetric shift of the final positions of the wave packets with respect to $x = 0$ (see panel (a)), which is a result of the distortion of the boundary between regions I and II (the final wave packets are not symmetrically distributed with respect to $x = 0$). This boundary evolves in time at the same constant velocity than the corresponding expected value of the velocity for the total superposition,

$$\bar{v}_A = \frac{\bar{p}_A}{m} = \frac{\langle \Psi_A^* | \hat{p} | \Psi_A \rangle}{m} = \frac{p_{01} + p_{02}}{2m}, \quad (43)$$

because both wave packets are identical and normalized (see Eq. (19)). In particular, since $p_{01} = 10$ and $p_{02} = -30$, we have $\bar{v}_A = -10$. Integrating the equation of motion $\dot{\bar{x}}_A = \bar{v}_A$ (according to Ehrenfest theorem [30]), we obtain

$$\bar{x}_A(t) = \bar{x}_0 + \bar{v}_A t, \quad (44)$$

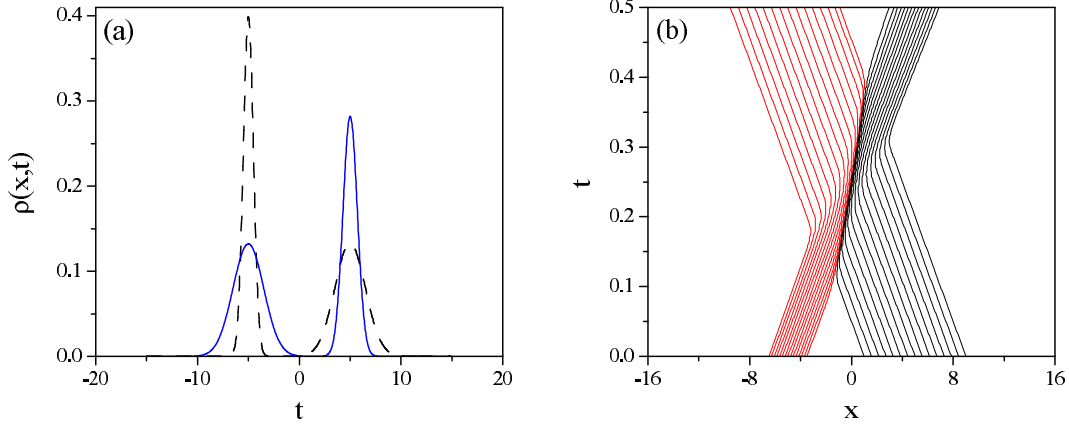


Figure 6. (a) Probability density at $t = 0$ (black-dashed line) and $t = 0.8$ (blue-solid line) for a wave packet superposition with $\sigma_{01} = 0.5$ and $\sigma_{02} = 1.5$. The value of the other relevant parameters are $|p_{01}| = |p_{02}| = 20$ and $\alpha = 1$. (b) Quantum trajectories associated with the dynamics described in the situation displayed in panel (a).

with $\bar{x}_0 = \langle \Psi^* | \hat{x} | \Psi \rangle = (x_{01} + x_{02})/2$. Equation (44) describes the time-evolution of the boundary between regions I and II in this case —note that for $p_{02} = -p_{01}$, we recover again the time-independent boundary found for identical wave packets, studied in the previous section. As expected, this boundary also defines the non-crossing line for the associate quantum trajectories, which forbids the trajectory transfer from one region to the other one and vice versa, as seen in Fig. 5(b). Because of this property, we find that the two wave packets behave like two classical particles undergoing an elastic scattering: there is only transfer (indeed, exchange) of momentum during the scattering process, but the net balance of probability is zero since no trajectories are transferred. Moreover, note that indeed this effect will not be noticeable unless one looks at the quantum trajectories —as seen in panel (a), the evolution of the wave packets does not provide any clue on it.

In case B, since both velocities are equal in modulus, after interference the centers of the outgoing wave packets occupy symmetric positions with respect to $x = 0$, as seen in Fig. 6(a) (only the different width disturbs the full symmetry). However, as in case A, the lack of total symmetry also causes the distortion of the boundary between regions I and II (see panel (b)), with a similar behavior regarding the non-crossing (or non-transfer) property. Now, since the modulus of both momenta are the same, $\langle \Psi^* | \hat{p} | \Psi \rangle = 0$ and therefore we cannot appeal to the same argument as before to explain this distortion effect. However, there is still a sort of effective “internal” momentum which depends on the ration between the widths of the wave packets. Assuming that the spreading is basically constant for the time we have propagated the trajectories, the corresponding effective velocity is given by

$$\bar{v}_B = \frac{\sigma_{01}^{-1} v_{01} + \sigma_{02}^{-1} v_{02}}{\sigma_{01}^{-1} + \sigma_{02}^{-1}} = \left(\frac{\sigma_{02} - \sigma_{01}}{\sigma_{01} + \sigma_{02}} \right) v_0, \quad (45)$$

with $v_{01} = v_0 = -v_{02}$ ($v_0 > 0$); since the width of the wave packets varies in time, a slight time-dependence can be expected in \bar{v}_B , although in our case, as can be noticed from Fig. 6(b), it can be neglected for practical purposes. Substituting the numerical values used in the propagation into (45), we find $\bar{v}_B = 5$. The boundary or non-crossing line will be then given by

$$\bar{x}_B(t) = \bar{x}_0 + \bar{v}_B t, \quad (46)$$

where

$$\bar{x}_0 = \frac{\sigma_{01}^{-1} x_{01} + \sigma_{02}^{-1} x_{02}}{\sigma_{01}^{-1} + \sigma_{02}^{-1}} = - \left(\frac{\sigma_{02} - \sigma_{01}}{\sigma_{01} + \sigma_{02}} \right) x_0, \quad (47)$$

with $x_{02} = -x_{01} = x_0$ ($x_0 > 0$) —note that, otherwise, $\bar{x}_0 = 0$, as infers from Fig. 6(a), since the larger width of one of the wave packets balances the effect of the larger height of the other one. Despite this internal redistribution or balance of momentum, it is clear that we find again, as in case A, an elastic collision-like behavior.

The effect of an effective internal momentum could be explained by considering that, in this case, the relative size of the wave packets acts like a sort of *quantum inertia* or effective mass. Consider the trajectories associated with the wave packet with smaller value of σ_0 (black trajectories in Fig. 6(b)). As can be noticed, it takes approximately 0.2 time units the whole swarm to leave the scattering or collision region (along the non-crossing boundary) —or, equivalently, to revert the sign of the momentum of all the trajectories constituting the swarm and get their final asymptotic momenta. On the other hand, the trajectories associated with the wave packet with larger σ_0 (red trajectories in Fig. 6(b)) revert their momenta much faster, in about 0.1 time units —of course, we are not considering here the time that trajectories remain moving along the boundary, since the total “interaction” time has to be the same for both swarms of trajectories. Thus, we find that the larger the spreading momentum, the larger also the quantum inertia of the swarm of particles to change the propagation momentum and, therefore, to reach the final state.

We would also like to note another interesting property associated with case B. Consider that both wave packets lack their corresponding normalizing factor A_t when introduced in the superposition. If we then compute the expected value of the momentum, for instance, we obtain

$$\langle \hat{p} \rangle_B = \frac{\langle \Psi_B^* | \hat{p} | \Psi_B \rangle}{\langle \Psi_B^* | \Psi_B \rangle} = \frac{\sigma_{01} v_{01} + \sigma_{02} v_{02}}{\sigma_{01} + \sigma_{02}} = \left(\frac{\sigma_{01} - \sigma_{02}}{\sigma_{01} + \sigma_{02}} \right) p_0, \quad (48)$$

i.e., there should be a certain “drift” towards region I, such as in case A —and the same holds if we compute instead the expected value of the position. Note that in the previous case the normalization of each Gaussian wave packet produces a balance: the probability with which each wave packet contributes to the superposition is the same ($c_1^2 = c_2^2 = 1/2$) because the width of one compensates the height of the other, as explained above. Therefore, the expected value of both position and momentum have to be zero. However, this compensation does not happen now: both wave packets have the

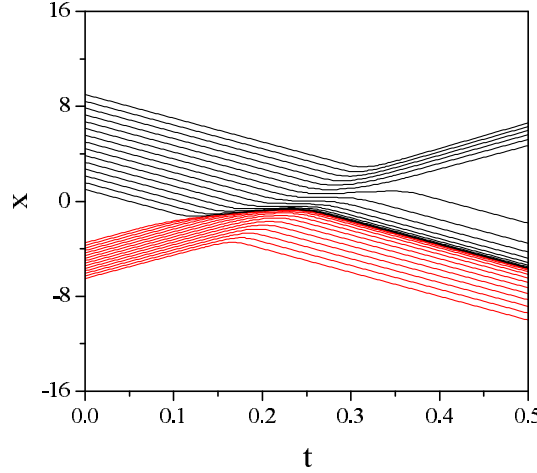


Figure 7. Bohmian trajectories associated with a Gaussian wave-packet superposition with $\sigma_{01} = 0.5$ and $\sigma_{02} = 1.5$. The value of the other relevant parameters are $p_{01} = -p_{02} = 20$ and $\alpha = 1$.

same height although their widths differ, thus contributing with different probabilities P to the superposition,

$$P_1 = \frac{\sigma_{01}}{\sigma_{01} + \sigma_{02}} \quad \text{and} \quad P_2 = \frac{\sigma_{02}}{\sigma_{01} + \sigma_{02}}, \quad (49)$$

which produce the results observed in Fig. 7 (again, we assume that $\sigma_t \approx \sigma_0$ for the time considered). However, by inspecting (48), we note that if we add the averaged momentum $\bar{p}_B = m\bar{v}_B$, the total average momentum vanishes. Somehow the averaging defined by (48) acts as in classical mechanics, when a certain magnitude (e.g., the position or the momentum) is computed with respect to the center of mass of a system. Here, \bar{p}_B is the magnitude necessary to reset the superposition of non normalized Gaussian wave packets to a certain ‘‘center of spreading’’. On the other hand, it is also important to stress the fact that, in this case, the clear boundary between the swarms of trajectories associated with each initial wave packet disappears. Now, although there is still a boundary, it does not prevent for the transfer of trajectories from one region to the other, as before. This effect, similar to consider inelastic scattering in classical mechanics, arises as a consequence of having wave packets with different probabilities, which we analyze below.

As seen above, unless there is an asymmetry in the probabilities carried by each partial wave in the superposition, there is always a well-defined boundary or non-crossing line between regions I and II. However, in the second example of case B, we have observed that it is enough an asymmetry in the probability distribution to break immediately the non-crossing line. Instead of using non normalized Gaussian wave packets, let us consider case C, which is equivalent although the asymmetry is caused by $\alpha \neq 1$ instead of the wave-packet normalization. As we have seen in the two previous cases, provided both wave packets have the same weight (or, at least, both contribute equally to the superposition), the corresponding quantum trajectories, even if they are evenly

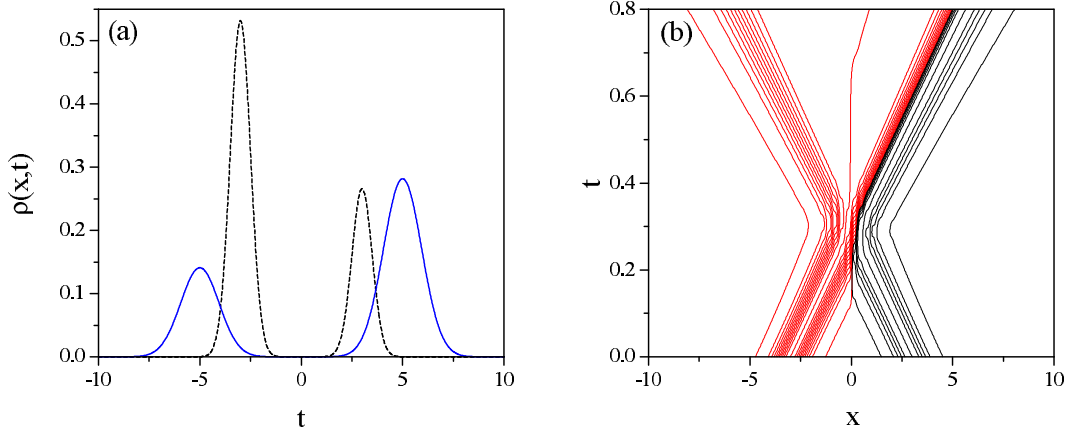


Figure 8. (a) Probability density at $t = 0$ (black-dashed line) and $t = 0.8$ (red-solid line) for a wave packet superposition with $\alpha = 0.5$ (i.e., $c_1^2 = 2/3$ and $c_2^2 = 1/3$). The value of the other relevant parameters are $p_{01} = -p_{02} = 10$ and $\sigma_{01} = \sigma_{02} = 0.5$. (b) Quantum trajectories associated with the dynamics described by the situation displayed in panel (a). The initial conditions for the quantum trajectories have been assigned by considering the different weights associated with each wave packet.

distributed (equidistant) along a certain distance initially, they are going to give a good account of the whole dynamics. However, if the weights change, the same does not hold anymore. Somehow equal weights (or equal probabilities) means the division of the coordinate space into two identical regions, each one influenced only by the corresponding wave packet. In other words, there are always two well-defined swarms of trajectories, each one associated with one of the initial wave packets. When the weights change, apparently we have something similar to what we have been observing until now: the wave packets exchange their positions (see Fig. 8(a)). However, when we look at the associate quantum trajectories, we realize that there is transfer or flow of trajectories from one of the initial swarms to the other one. This transfer takes place from the swarm with larger weight to the lesser one, thus distorting importantly the boundary between regions I and II, as seen in Fig. 8(b), where this boundary lies somewhere between the two trajectories represented in blue (the trajectories that are closer to $x = 0$ in each swarm). However, note that this does not imply that the number of trajectories varies in each region asymptotically, but only the number of them belonging to one or the other wave packet. Thus, if initially we have $N_1 \propto c_1^2$ trajectories associated with ψ_1 and $N_2 \propto c_2^2$ with ψ_2 , asymptotically we will observe $N'_1 = (1-\alpha)N_1 \propto c_2^2$ and $N'_2 = N_2 + \alpha N_1 \propto c_1^2$ due to the trajectory transfer. Unlike the two previous cases discussed above, this process can be then compared with inelastic scattering, where, after collision, not only the probability fluxes but also the number of particles changes. Accordingly, it is also important to mention that, due to the trajectory transfer, representations with evenly distributed trajectories are not going to provide a good picture of the problem dynamics, as infers from Fig. 7. Rather, we can proceed in two different ways. The obvious procedure is to consider initial positions

distributed according to the corresponding (initial) probability densities. This procedure carries a difficulty: the number of trajectories needed to have a good representation of the dynamics may increase enormously depending on the relative weights. The second procedure is to consider evenly spaced values of the probability density and allocate at such space points the initial positions of the trajectories, as we have done to construct Fig. 8(b). In this case, although the trajectories will not accumulate exactly along the regions with larger values of the probability density, this construction has the advantage that we can follow the transport of equi-spaced probabilities along each particular trajectory. To make more apparent the difference in the relative number of trajectories (probability density) associated with each initial wave packets, we have considered $N_1 = 23$ and $N_2 = 11$ (i.e., $N_2/N_1 \sim 0.48 \approx c_2^2/c_1^2 = 0.5$). After scattering, the numbers that we have are $N'_1 = 11$ and $N'_2 = 23$, which are in the expected ratio $c'_2/c'_1 = c_2^2/c_1^2 = 2$.

As said at the beginning of this subsection, here we have only considered the collision-like case. The same kind of results are expected for the analogous diffraction-like cases, with the addition that they manifest as a loss of fringe visibility. Thus, for cases A and B, one could appreciate a well define non-crossing line and a loss of fringe visibility due to the divergent velocities, v_p and v_s , respectively. And, for case C (or the second example in case B), the loss of fringe visibility would be caused by the transfer of trajectories, which would also lead to the distortion of the non-crossing line.

3.4. Coherent superpositions, potential barriers and resonances

Finally, here we are going to analyze an interesting effect associated with the non-crossing property described in the previous sections. Consider a Gaussian wave packet scattered off an impenetrable potential wall (for simplicity, we will assume $v_p > v_s$ for now). After some time the wave packet will collide with the wall and then part of it will bounce backwards. The interference of the forward (f) and backward (b) wave packets will lead to a fringe-like pattern similar to those observed in the previous sections (see red-solid line in Fig. 9(a)), with also a time, t_{\max}^{int} , for which the interference fringes are maximally resolved. Putting aside the initial Gaussian shape of the wave packet (and, therefore, the effects associated with v_s), if this process is represented as

$$\Psi = \psi_f + \psi_b \sim e^{imv_p x/\hbar} + e^{-imv_p x/\hbar} \quad (50)$$

at t_{\max}^{int} , we obtain $\rho(x) \sim \cos^2(mv_p x/\hbar)$. The distance between two consecutive minima is then $w_0 = \pi\hbar/mv_p$, which turns out to be the same distance between two consecutive minima in the two wave-packet interference process (see black-dashed line in Fig. 9(a)). That is, although each process has a different physical origin (barrier scattering *vs* wave packet collision), the effect is similar —there is a certain shift in the position of the corresponding maxima ($\sim \pi/2$), which arises from the fact that, in the case of barrier scattering, the impenetrable wall forces the wave function to have a node at $x = 0$. If now we go to the corresponding quantum trajectories, we observe (see Fig. 9(b), with red-solid line) that as the wave packet starts to “feel” the presence of the wall, the

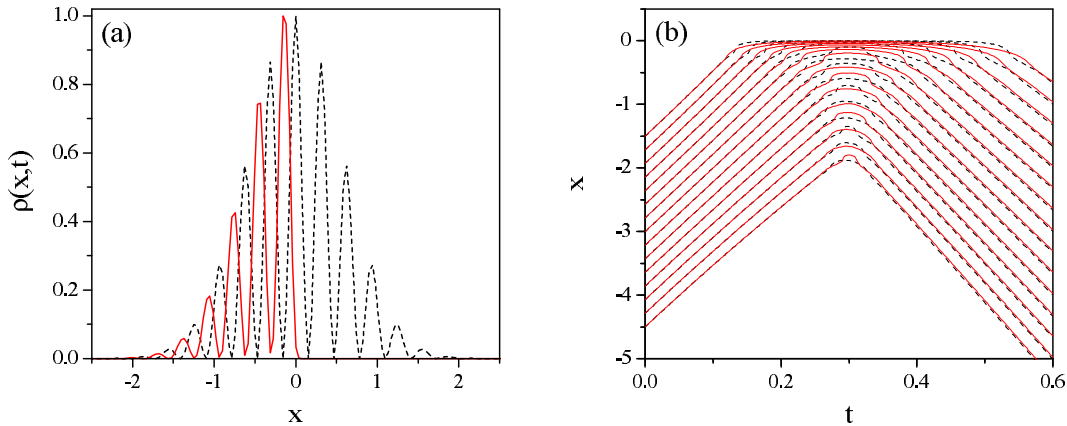


Figure 9. (a) Probability density at $t = 0.3$ for the collision of a Gaussian wave packet off: an external impenetrable wall (red-solid line) and another (identical) Gaussian wave packet (black-dashed line). To compare, the maxima of both probability densities are normalized to unity. (b) Bohmian trajectories illustrating the dynamics associated with the two cases displayed in part (a). Here, $v_p = 10$ and $v_s = 1$.

trajectories bend gradually (in the x vs t representation) and then start to move in the opposite direction. When these trajectories are compared with those associated with the problem of the two wave-packet superposition, the resemblance between trajectories with the same initial positions is excellent, except in the interference region due to the different location of the nodes of the corresponding wave functions —these differences are the trajectory counterpart of the shift mentioned before.

From the previous description one might infer that, since the dynamics for $x < 0$ and for $x > 0$ do not mix (due to non-crossing), each half of the central interference maximum arises from different groups of trajectories. Thus, in principle, one should be able to arrange the impenetrable wall problem in such a way that allows us to explain this effect. Within this context, although all the peaks have the same width as in the wave-packet superposition problem, the closest one to the wall should have half such a width, i.e., $w \sim \pi\hbar/2p = w_0/2$. Due to boundary conditions and the forward-backward interference discussed above, it is clear that this peak cannot arise from interference, but from another mechanism: a *resonance* process. Therefore, apart from the wall, we also need to consider the presence of a potential well. In order to observe a resonance or bound state, the width of this well should be, at least, of the order of the width w of the bound state. From standard quantum mechanics [30], we know that in problems related to bound states in finite well potentials the relationship

$$V_0 a^2 = n \frac{\hbar^2}{2m} \quad (51)$$

always appears, where a is the half-width of the well ($a = w/2$) and n is an integer number. The eventual solutions (bound states) are then observable or not depending on whether the condition which it might correspond will be in consonance or not with this condition. In our case, we can use (51) to obtain an estimate of the well depth,

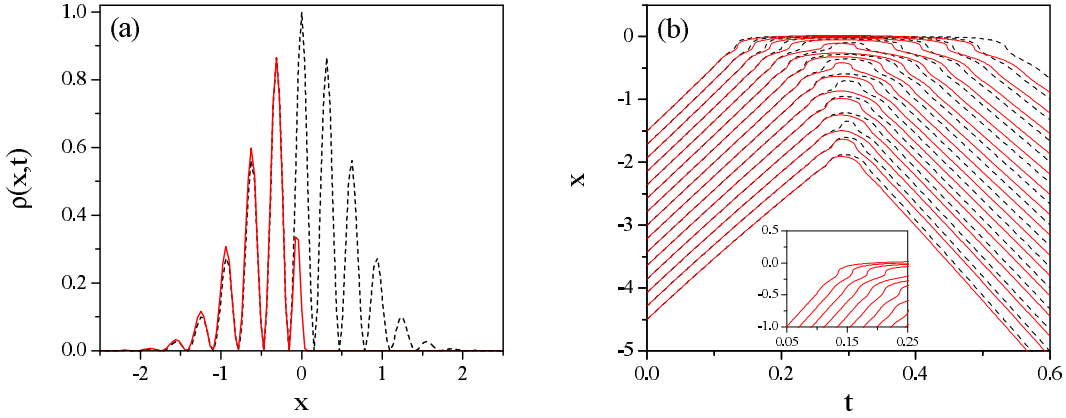


Figure 10. (a) Probability density at $t = 0.3$ for the collision of a Gaussian wave packet off: the external potential described by Eq. (53) (red-solid line) and another (identical) Gaussian wave packet (black-dashed line). To compare, the maxima at $x \approx -0.32$ of both probability densities are normalized to the same height (the maximum at $x = 0$ of the two wave packet probability density being set to unity). (b) Bohmian trajectories illustrating the dynamics associated with the two cases displayed in part (a). Inset: enlargement of the plot around $t = 0.15$ to show the action of the potential well on the trajectories started closer to $x = 0$. Here, $v_p = 10$ and $v_s = 1$.

which results

$$V_0 = \frac{16}{\pi^2} \frac{p^2}{2m} \quad (52)$$

when we assume $n = 1$. Now, we have then a potential which presents a short-range attractive well before reaching the impenetrable wall,

$$V(x) = \begin{cases} 0 & x < -w \\ -V_0 & -w \leq x \leq 0 \\ \infty & 0 < x \end{cases} . \quad (53)$$

If we compute now $\rho(\mathbf{r}, t)$ at t_{\max}^{int} , we obtain the result displayed in Fig. 10(a). As can be noticed, now there is an excellent matching of the peak widths, with the closest one to the wall being half-width when compared with the remaining ones —the associate quantum trajectories are displayed and compared in Fig. 10(b).

The equivalence between the two wave packet collisions and the scattering of a wave packet off a potential is not restricted to the condition $v_p > v_s$, but it is of general validity. As shown in Fig. 6, it also holds for the diffraction-like situation, i.e., $v_p < v_s$. In Fig. 11(a), we show that half of the diffraction-like pattern is again well reproduced after replacing one of the wave packets by an external potential, and the same also happens for the corresponding quantum trajectories (see Fig. 11(b)). However, in order to find these results, now a subtlety has to be considered: the central diffraction maximum increases its width with time. In terms of simulating this effect with a potential function, it is clear that the width of the potential well should also increase with time. Thus, we need to consider a “dynamical” or time-dependent potential function rather than a static

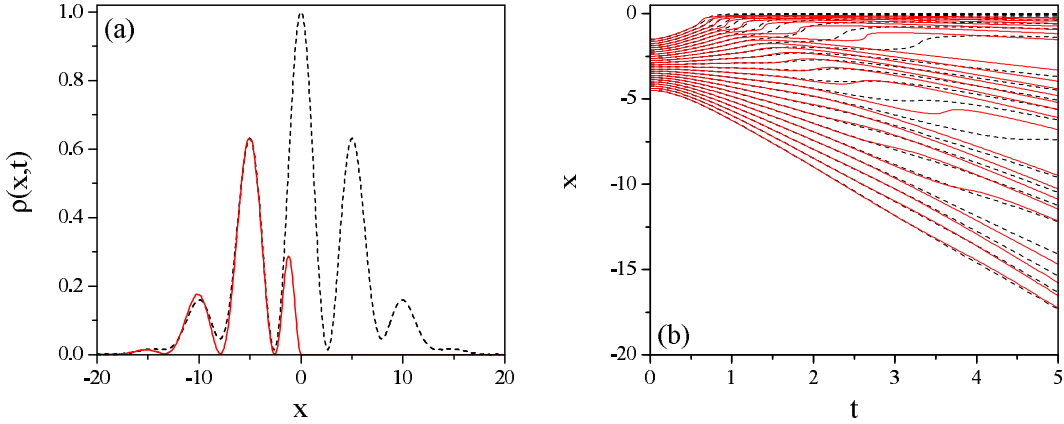


Figure 11. (a) Probability density at $t = 5$ for the collision of a Gaussian wave packet off: the external, time-dependent potential described by Eq. (53) (red-solid line) and another (identical) Gaussian wave packet (black-dashed line). To compare, the maxima at $x \approx -5$ of both probability densities are normalized to the same height (the maximum at $x = 0$ of the two wave packet probability density being set to unity). (b) Bohmian trajectories illustrating the dynamics associated with the two cases displayed in part (a). Here, $v_p = 0.1$ and $v_s = 1$.

one, as done before. In order to determine this potential function, we proceed as before. First, we note that the two wave-packet collision problem, Eq. (29), is explicitly written in terms of Gaussian wave packets (see Eq. (19)) as

$$\Psi \sim e^{-(x+x_t)^2/4\sigma_t\sigma_0+ip(x+x_t)/\hbar+iEt/\hbar} + e^{-(x-x_t)^2/4\sigma_t\sigma_0-ip(x-x_t)/\hbar+iEt/\hbar}, \quad (54)$$

where

$$x_t = x_0 - v_p t \quad (55)$$

(for simplicity, we have neglected the time-dependent prefactor, since it is not going to play any important role regarding either the probability density or the quantum trajectories). The probability density associated with (54) is

$$\rho(x, t) \sim e^{-(x+x_t^2)/2\sigma_t^2} + e^{-(x-x_t^2)/2\sigma_t^2} + 2e^{-(x^2+x_t^2)/2\sigma_t^2} \cos[f(t)x], \quad (56)$$

with

$$f(t) \equiv \frac{\hbar t}{2m\sigma_0^2} \frac{x_t}{\sigma_t^2} + \frac{2p}{\hbar}. \quad (57)$$

As can be noticed, (56) is maximum when the cosine is $+1$ (constructive interference) and minimum when it is -1 (destructive interference). The first minimum (with respect to $x = 0$) is then reached when $f(t)x = \pi$, i.e.,

$$x_{\min}(t) = \frac{\pi}{\frac{2p}{\hbar} + \frac{\hbar t}{2m\sigma_0^2} \frac{x_t}{\sigma_t^2}} = \frac{\pi\sigma_t^2}{\frac{2p\sigma_0^2}{\hbar} + \frac{\hbar t}{2m\sigma_0^2} x_0}, \quad (58)$$

for which

$$\rho[x_{\min}(t)] \sim 4e^{-(x_{\min}^2+x_t^2)/2\sigma_t^2} \sinh\left(\frac{x_{\min}x_t}{2\sigma_t^2}\right), \quad (59)$$

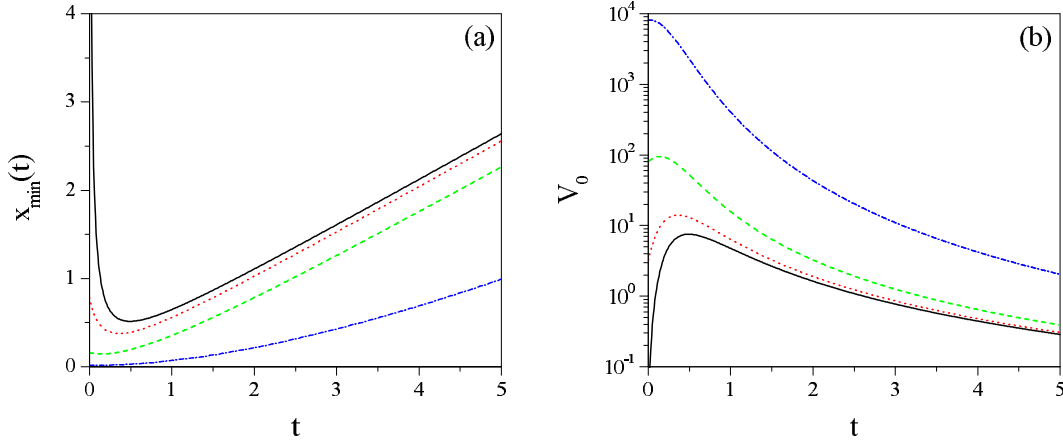


Figure 12. (a) Plot of $x_{\min}(t)$ as a function of time for different values of the propagation velocity: $v_p = 0.1$ (black solid line), $v_p = 2$ (red dotted line), $v_p = 10$ (green dashed line) and $v_p = 100$ (blue dash-dotted line). (b) Plot of V_0 as a function of time for the same four values of v_p considered in panel (a). In all cases, $v_s = 1$.

which basically is zero if the initial distance between the two wave packets is relatively large when compared with their spreading.

In Fig. 12(a), we can see the function $x_{\min}(t)$ for different values of the propagation velocity v_p . As seen, $x_{\min}(t)$ decreases with time up to a certain value, and then increases again, reaching a linear asymptotic behavior. From (58) we find that the minimum value of $x_{\min}(t)$ is reached at

$$t_{\min} = \frac{4m\sigma_0^4}{\hbar^2 x_0} \left[-p + \sqrt{p^2 + p_s^2 \left(\frac{x_0}{\sigma_0} \right)^2} \right]. \quad (60)$$

The linear time-dependence at long times is characteristic of the Fraunhofer regime, where the width of the interference peaks increases linearly with time. On the other hand, the fact that, at $t = 0$, $x_{\min}(t)$ increases as v_p decreases (with respect to v_s) could be understood as a “measure” of the coherence between the two wave packets, i.e., how important the interference among them is when they are far apart (remember that, despite their initial distance, there is always an oscillating term in between due to their coherence [31]). Note that this is in accordance with the standard quantum-mechanical arguments that interference-like patterns are manifestations of the wavy nature of particles, while scattering-like ones display their corpuscle nature (more classical-like). Thus, as the particle becomes more “quantum-mechanically”, the initial reaching of the “effective” potential well should be larger. And, as the particle behaves in a more classical fashion, this reaching should decrease and be only relevant near the scattering or interaction region, around $x = 0$. From Eq. (58), two limits are thus worth discussing. In the limit $p \sim 0$,

$$x_{\min}(t) \approx \frac{\pi\sigma_t^2 \tau}{x_0 t} \quad (61)$$

and $t_{\min} \approx \tau$. In the long-time limit, this expression becomes $x_{\min}(t) \approx (\pi\hbar/2m)(t/x_0)$, i.e., x_{\min} increases linearly with time, as mentioned above. On the other hand, in the limit of large σ_0 (or, equivalently, $v_p \gg v_s$),

$$x_{\min}(t) \approx \frac{\pi\hbar}{2p} \quad (62)$$

and $t_{\min} \approx 0$. That is, the width of the “effective” potential barrier remains constant in time, this justifying our former hypothesis above, in the scattering-like process, when we considered $w \sim \pi\hbar/2p$.

After Eq. (58), the time-dependent “effective” potential barrier is defined as (53),

$$V(t) = \begin{cases} 0 & x < x_{\min}(t) \\ -V_0[x_{\min}(t)] & x_{\min}(t) \leq x \leq 0 \\ \infty & 0 < x \end{cases} . \quad (63)$$

with the (time-dependent) well depth being

$$V_0[x_{\min}(t)] = \frac{2\hbar^2}{m} \frac{1}{x_{\min}^2(t)} . \quad (64)$$

The variation of the well depth along time is plotted in Fig. 12(a) for the different values of v_p considered in Fig. 12(b). As seen, the well depth increases with v_p (in the same way that its width, x_{\min} , decreases with it) and decreases with time. For low values of v_p , there is a maximum, which indicates the formation of the bound state that will give rise to the innermost interference peak (with half the width of the remaining peaks, as shown in Fig. 11(a)). Note that, despite the time-dependence of the well depth, in the limit $v_p \gg v_s$, we recover Eq. (52).

We have shown that the problem of the interference of two colliding wave packets can be substituted by the problem of the collision of a wave packet off a potential barrier. Although the model that we have presented is very simple, it is important to stress that it reproduces fairly well the dynamics involved —of course, one can always search for more refined and precise models. The fact that one can make this kind of substitutions puts quantum mechanics and the superposition principle on the same grounds as two important frameworks in classical physics (one could think of many other situations, but these two ones are particularly general and well known). The first one is widely used in classical mechanics (and then, in its quantized version, also in quantum mechanics): it is the equivalence between a two-body problem and a one-body problem acted by a central force. As can be noticed, our reduction is of the same kind: a two wave-packet dynamical process can be reduced to the dynamics of a single wave packet subjected to the action of an external potential. The second framework is the one provided by the so-called method of images, widely used in electrostatics: the interaction between a charge distribution and a conductor can be replaced by the interaction between such a charge distribution and another virtual one. This would be the reciprocal situation to ours: the dynamics induced by an external potential on a wave packet can be translated as the dynamics taking place when two wave packets (ours and a virtual one) are considered.

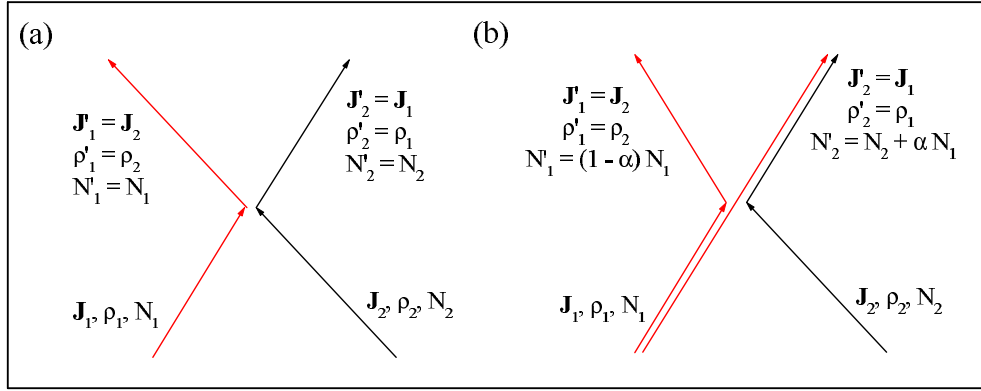


Figure 13. Schematic representation of the two types of processes that may take place in two wave-packet collisions: (a) elastic-like scattering and (b) inelastic-like scattering. See text for details.

4. Final discussion and conclusions

Here we have presented a detailed analysis of quantum interference within the framework of quantum trajectories. As we have shown, there are at least two important effects which are masked when interference is studied from the standard point of view, but that become apparent as soon as we move to the Bohmian domain: (a) it is always possible to determine uniquely the departure region of a particle from the final outcome, and (b) interference can be described as an effect similar to that of a collision with an effective potential barrier. Bohmian trajectories allow one to determine the origin of the particles that contribute to each final wave packet, contrary to the standard view of interference processes, where the finally wave packets are commonly associated with the time-evolved initial ones, according to the superposition principle. In other words, effect (a) can be regarded as a sort of distinguishability, which should not be confused with that one arising when one considers identical particles. This issue is connected with the effect (b) in the sense that it allows us to describe the process, in the collision-like case, as classical collisions. Two situations can then happen. If the probability is equi-distributed between the two wave packets, the effect is similar to classical elastic particle-particle collisions, where only the momentum is transferred. In our case, what is transferred is the probability distribution through the probability density current, since the number of particles associated with each wave packet remains the same. This situation, represented schematically in Fig. 13(a), corresponds to the cases A and the first one B described in section 3.3. On the other hand, when the probabilities are asymmetrically distributed, there is a probability transfer which translates into a trajectory transfer —the well defined non-crossing line then disappears. This behavior, which is similar to a classical inelastic particle-particle collision, is displayed in Fig. 13(b) and corresponds to the case C and the second example B (see section 3.3).

Observing collision-like behaviors or not depends on whether the relative spreading velocity of each wave packet is larger than the velocity associated with their propagation.

We have seen that, if the propagation velocity is larger than the spreading one, one will observe collision-like behaviors. In other words, the wave packets behave like classical particles or *corpuscles* to some extent. Of course, note that when we use the concept “collision”, we are not referring exactly to a true particle-particle collision, since the two wave packets indeed refer to the *same* system (which, by means of some procedure, as described above, has been split). On the other hand, when the spreading velocities dominate the dynamics, the behavior is diffraction-like, i.e., the wave packets behave in a wavy manner, giving rise to diffraction patterns after their interference.

Finally, it is also very interesting the fact that wave packet interference problems can be understood within the context of scattering of effective potential barriers. That is, in the same way that in classical mechanics one can substitute a particle-particle problem by that of an effective particle (associated with the center of the mass of the particle-particle system) acted by an (also effective) interaction central potential, here we have shown that the interference process can also be rearranged in such a way that instead of considering two wave packets, one can consider the scattering of a wave packet by an effective (time-dependent) potential barrier. In this sense, it is interesting to note that this could be considered the seed of refined and well-known methods used to deal with many body systems, where the many degrees of freedom are replaced by a sort of effective time-dependent potentials [32]. It is worth stressing that, in order to describe properly the interference fringes during the process, we have shown that these potentials have to support bound states or resonances. Of course, in those cases where the non-crossing boundary disappears because the probability is not equally distributed between the two wave packets, the impenetrable barriers have to be replaced by transparent or step barriers. Then, in the same way that after the collision process part of the trajectories associated with one of the wave packets attaches to the other one, after the collision with the transparent barrier part of the trajectories will move along the barrier.

Acknowledgments

This work has been supported by the Ministerio de Ciencia e Innovación (Spain) under Project No. FIS2007-62006. A.S. Sanz also acknowledges the Consejo Superior de Investigaciones Científicas (Spain) for a JAE-Doc contract.

References

- [1] Macchiavello C, Palma G M and Zeilinger A (eds.) 1999 *Quantum Computation and Quantum Information Theory* (Singapore: World Scientific)
- [2] Nielsen M A and Chuang I L 2000 *Quantum Computation and Quantum Information* (Cambridge: Cambridge University Press)
- [3] Brumer P W and Shapiro M 2003 *Principles of the Quantum Control of Molecular Processes* (Hoboken, NJ: Wiley-Interscience)
- [4] Schrödinger E 1935 *Proc. Cam. Phil. Soc.* **31** 555
- [5] See also:
Schrödinger E 1936 *Proc. Cam. Phil. Soc.* **32** 446;

Einstein A, Podolsky B and Rosen N 1935 *Phys. Rev.* **47** 777;
 Bohm D 1951 *Quantum Mechanics* (New York: Dover)

[6] Feynman R P, Leighton R B and Sands M 1965 *Quantum Mechanics, The Feynman Lectures on Physics*, Vol. 3 (Reading, MA: Addison-Wesley)

[7] Scalapino D J 1969 in *Tunneling Phenomena in Solids*, E Burstein and S Lundqvist (eds.) (New York: Plenum) p. 447

[8] Berman P R (ed.) 1997 *Atom Interferometry* (San Diego: Academic Press)

[9] Shin Y, Saba M, Pasquini T A, Ketterle W, Pritchard D E and Leanhardt A E 2004 *Phys. Rev. Lett.* **92**, 050405

[10] Zhang M, Zhang P, Chapman M S and You L 2006 *Phys. Rev. Lett.* **97** 070403

[11] Cederbaum L S, Streltsov A I, Band Y B and Alon O E 2007 *Phys. Rev. Lett.* **98** 110405

[12] Hänsel W, Reichel J, Hommelhoff P and Hänsch T W 2001 *Phys. Rev. Lett.* **86** 608;
 Hänsel W, Reichel J, Hommelhoff P and Hänsch T W 2001 *Phys. Rev. A* **64** 063607

[13] Hinds E A, Vale C J and Boshier M G 2001 *Phys. Rev. Lett.* **86** 1462

[14] Andersson E, Calarco T, Folman R, Andersson M, Hessmo B and Schmiedmayer J 2002 *Phys. Rev. Lett.* **88** 100401

[15] Kapale K T and Dowling J P 1995 *Phys. Rev. Lett.* **95** 173601;
 Thanvanthri S, Kapale K T and Dowling J P 2008 e-print arXiv:0803.2725v1 (quant-ph)
Arbitrary Coherent Superpositions of Quantized Vortices in Bose-Einstein Condensates from Orbital Angular Momentum Beams of Light

[16] Chapman M S, Ekstrom C R, Hammond T D, Schmiedmayer J, Tannian B E, Wehinger S and Pritchard D E 1995 *Phys. Rev. A* **51** R14

[17] Deng L, Hagley E W, Denschlag J, Simsarian J E, Edwards M, Clark C W, Helmerson K, Rolston S L and Phillips W D 1999 *Phys. Rev. Lett.* **83** 5407

[18] Bohm D 1952 *Phys. Rev.* **85** 166, 180

[19] Holland P R 1993 *The Quantum Theory of Motion* (Cambridge: Cambridge University Press)

[20] Sanz A S, Borondo F and Miret-Artés S 2002 *J. Phys.: Condens. Matter* **14** 6109

[21] Sanz A S and Miret-Artés S 2007 *J. Chem. Phys.* **126** 234106

[22] Wyatt R E 2005 *Quantum Dynamics with Trajectories* (New York: Springer)

[23] Berry M V and Balazs N L 1979 *Am. J. Phys.* **47** 264;
 Unnikrishnan K and Rau A R P *Am. J. Phys.* **64** 1034;
 Siviloglou G A, Broky J, Dogariu A and Christodoulides D N 2007 *Phys. Rev. Lett.* **99** 213901

[24] Born M 1926 *Z. Physik* **37** 863;
 Born M 1926 *Z. Physik* **38** 803

[25] Madelung E 1926 *Z. Phys.* **40** 332

[26] Berry M V 1996 *J. Phys. A: Math. Gen.* **29** 6617;
 Hall M J W, Reineker M S and Schleich W P 1999 *J. Phys. A: Math. Gen.* **32** 8275;
 Wójcik D, Bialynicki-Birula I and Zyczkowski K 2000 *Phys. Rev. Lett.* **85** 5022

[27] Sanz A S 2005 *J. Phys. A: Math. Gen.* **38** 6037

[28] Sanz A S and Miret-Artés S 2007 *Chem. Phys. Lett.* **445** 350

[29] Sanz A S, Borondo F and Miret-Artés S 2000 *Phys. Rev. B* **61** 7743

[30] Schiff L I 1968 *Quantum Mechanics* (Singapore: McGraw-Hill) 3rd Ed

[31] Sanz A S and Miret-Artés S 2008 *Chem. Phys. Lett.* **458** 239

[32] Sanz A S, Giménez X, Bofill J M and Miret-Artés S 2008 *Time-Dependent Density Functional Theory from a Bohmian Perspective*, in *Theory of Chemical Reactivity*, P Chattaraj (ed.) (New York: Francis and Taylor)